1-2023

Design of Block Copolymer with Tunable Hydrophobic/Hydrophilic/Fluorophilic Interactions

Tatiane de Fatima Dutra

Abstract

Block copolymers (BCP) with balanced interactions and their resultant bulk-phase self-assembly have become increasingly important in advancing nanotechnology, separation, and energy applications. However, a few reports have addressed the synthesis challenge and bulk-phase self-assembly of such triblock copolymers. This thesis presents a facile route for preparing triblock copolymer via controlled radical and organocatalytic ring-opening polymerization that allows precise control over the incorporation of individual moieties in resultant polymer, responsible for balanced hydrophilic, hydrophobic/lipophilic, and fluorophilic interactions. Synthesized polymer with suggested self-assembled 2D lamellar nanostructure exhibits high-temperature stability. The long-term goal of this work is to selectively use this polymer class as a sorbent of adsorbing poly and perfluoro alkyl substances (PFAS) and gain a mechanistic understanding of interfacial phenomena.

MONTCLAIR STATE UNIVERSITY

Design of Block Copolymer with Tunable

Hydrophobic/Hydrophilic/Fluorophilic Interactions

by

Tatiane de Fatima Dutra

A Master's Thesis submitted to the faculty of

Montclair State University

In Partial Fulfillment of the Requirements

For the Degree of

Master of Science
January 2023

College of Science and Mathematics

Department of Chemistry & Biochemistry

Thesis Committee:

Dr. Amrita Sarkar
(Thesis Sponsor)

Dr. Magnus Bebbington
(Thesis Committee)

Dr. Nina Goodey
(Thesis Committee)

Dr. Jim Dyer
(Thesis Committee)

Design of Block Copolymer with Tunable

Hydrophobic/Hydrophilic/Fluorophilic Interactions

A THESIS

Submitted in partial fulfillment of the requirements

For the degree of Master of Science

by

TATIANE DE FATIMA DUTRA

Montclair State University

Montclair, NJ

2023

Acknowledgment

I want to thank my supervisor – Professor Amrita Sarkar, for her invaluable supervision and support during my MS degree. My gratitude extends to the financial support from National Science Foundation (CBET-2138438). I want to thank Professor Nina Goodey and Professor Magnus Bebbington for their help and advice. I also thank Professor Jim Dyer for his mentorship. I want to thank my friends and family in the United States for all their support and always believing in me. My appreciation also goes out to my family and friends in Brazil, especially to my father for his encouragement and loving support throughout all my studies.

Table of Contents:

List of Figures

List of Tables

Introduction & Motivation

Block copolymers (BCP) are a class of macromolecules combining two or more chemically dissimilar homopolymers via a covalent bond. BCPs are seen with variable architectures, including linear, graft, or segmented copolymer with linear backbone and branching, star, and cyclic. Covalently bonded, the chemically dissimilar blocks can undergo microphase separation resulting in various ordered nanoscale morphologies with a length scale of 5-100 nm; this feature is termed self-assembly.[1-5] Self-assembly phenomena are primarily governed by three parameters: (1) volume fraction of each block (ϕ), (2) total degree of polymerization or chain length (N), and (3) Flory-Huggins interaction parameter (χ).[2,3,6] Thermodynamic behavior of polymer melt is described by Flory-Huggins theory, where the enthalpy or entropy of each chain depends on the sum of interactions or conformations along the chain. The interaction between each segment is described as χ which is estimated by a semi-empirical equation (1.1), where δ is the Hildebrand solubility parameters for each block, V_{ref} is the per unit volume, k_B is Boltzman constant, and $k_B T$ is the thermal energy. As the mixing enthalpy is proportional to the N, the product χN describes the thermodynamic incompatibility between each block. The effective value of χN could be controlled easily by changing the average number of N.

$$\chi_{ij} = \frac{V_{ref} \times \left(\delta_i - \delta_j \right)^2}{k_B T}$$

(1.1)

During microphase separation, incompatible blocks separate from each other and tend to adopt nanoscale morphologies to minimize interfacial area by lowering total interfacial energy. Separately, chain stretching contributes significantly by maximizing conformational entropy. To produce the nanoscale phase structures shown in **Figure 1**, the BCP must approach the strong segregation limit $(SSL>>10.5)^{6,}$ where the χN would be significantly large. In contrast, the BCP with small χN approaches toward weak segregation limit (WSL<10) produces a disordered phase or phases with a lack of long-range ordering/poor ordering. By applying these assumptions, a theoretical phase diagram can be constructed, which predicts the equilibrium morphologies for an AB diblock copolymer. However, the complexity and number of morphologies increase upon incorporating the third block into AB linear BCP. Thus, three-dimensional network nanostructures such as alternating gyroid, bicontinuous gyroid, and another complex plethora of nanostructures, including core-shell cylinders, cylinders in lamellae, non-centrosymmetric lamellar, and chiral cylinders are found or predicted in ABC triblock copolymer, presented in **Figure 2**.[9-22] This more extensive collection of nanostructures is the result of increased numbers of molecular parameters, such as volume fractions of two blocks (ϕ_A, ϕ_B) and three interactions parameters ($\chi_{AB}N$, $\chi_{BC}N$, $\chi_{AC}N$). Polymer volume fractions are typically calculated based on the molar mass and densities of each homopolymer, whereas the interaction parameters are the product of interfacial energy and the total chain length. In addition, adding a third block introduces three unique sequences of ABC, ACB, and CAB, whereas one can expect one unique sequence for AB (AB = BA) only.
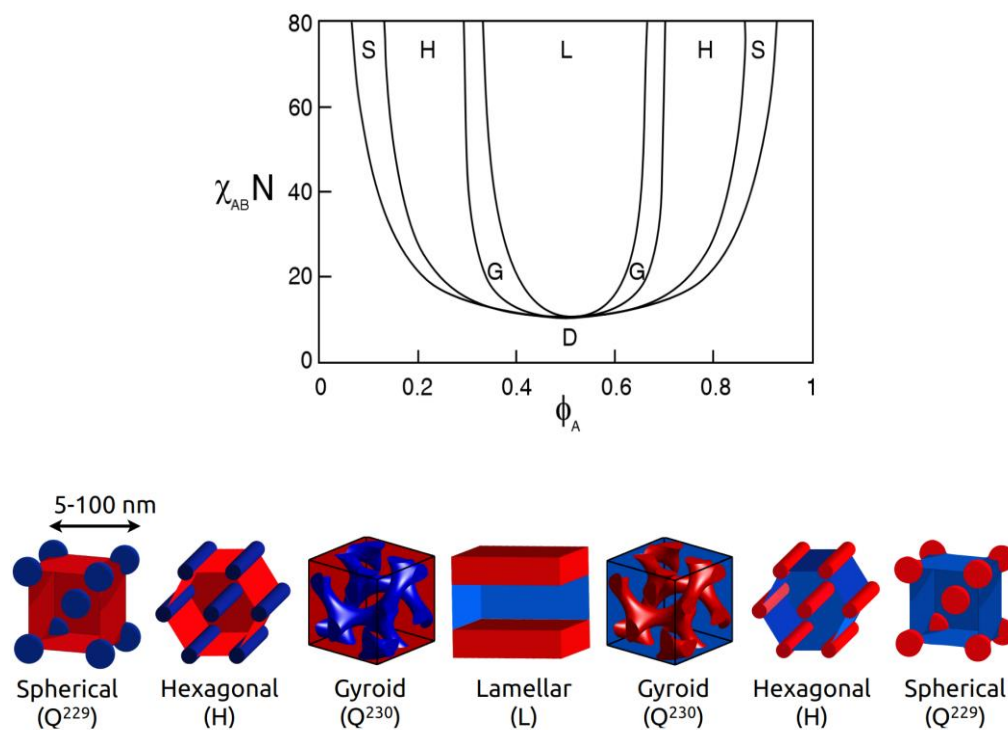
Figure 1. BCP phase diagram (theoretically predicted)[7,8] as a function of volume fraction of one block (φ). A block is chosen for **Figure 1**. Self-assembled (self-assembly in bulk) nanostructures obtained from diblock copolymer, including sphere (S), hexagonal (H), gyroid (G), lamellar (L), and disordered (D), are shown. Strong SSL is required to produce equilibrium morphologies, as depicted in the above figure. The morphologies depend on φ of each block and N of the total polymer, as χN controls such morphologies.

In recent years, a class of ABC triblock copolymer with a unique composition of moieties having hydrophilic, hydrophobic/lipophilic, and fluorophilic interactions got significant attention as it offers more advanced and exotic nanostructures compared to traditional ABC polymer due to its fast microphase separation in bulk and solution phases.[23-35] These structures are desirable for applications such as drug delivery, coating formulations, nanotechnology, and marine Antifouling/ Fouling-Release.[35-40] Additionally, fluorinated polymers are also desirable contrast reagents for the ^{19}F magnetic resonance imaging process (MRI).[36]
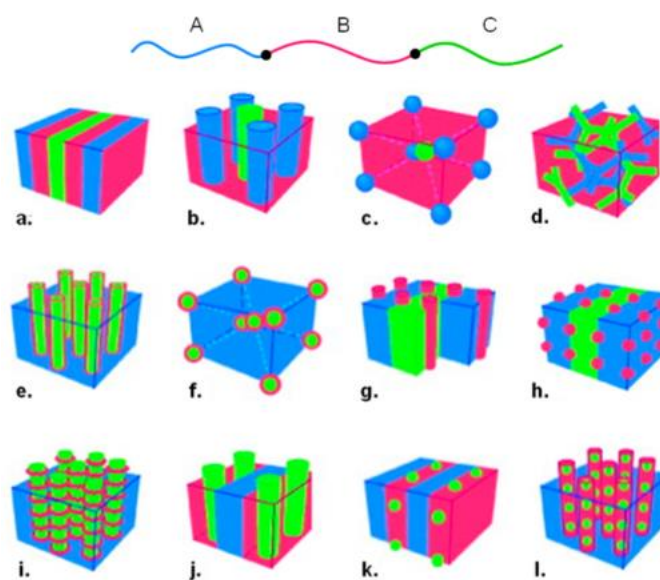
Figure 2. Potential equilibrium morphologies for linear ABC triblock terpolymer adapted from reference 22 with permission from references 10 and 21.

However, the self-assembly of such triphilic polymers in the solution/aquatic phase is well documented in the literature compared to bulk phases, which leads to the formation of dispersed organized objects such as micelles. Multicompartment micelles are the most well-known solution phase structure produced from linear triphilic polymers and reported to be used in various applications, including drug delivery, catalysts, and nanotechnology.[23,30] For example, Mohwald and coworker[25] reported a pentablock copolymer (PEO-*b*-PBLG-*b*-PFPE-*b*-PBLG-*b*-PEO) having two hydrophilic poly (ethylene oxide) blocks, two hydrophobic poly (y-benzyl L-glutamate) blocks, and a poly (perfluoro ether) block. These blocks' high immiscibility and hydrophobicity allow their self-assembly into spherical and cylindrical micelles with lengths ranging from 100 to 200 nm.[25] Likewise, Laschewsky et al. reported the multicompartment micelle formed from a long cationic hydrophilic block composed of poly(4-methyl-4-(4-vinyl benzyl)

morpholin-4-ium) (PVBM) represented by the light gray color in **Figure 3** and two short

hydrophobic blocks; a hydrocarbon one composed of polystyrene (PS), and a mixed

fluorocarbon/hydrocarbon block poly-(pentafluoro phenyl 4-vinyl benzyl ether) (PVBFP)

represented by the black spheres and the darker gray core, respectively on **Figure 3**.[37]

Both works showed logical design choices for achieving the strong incompatibility

between the blocks that favors segregation into distinct domains and leads into formation

of multi-compartments in resultant micelle nanostructures.
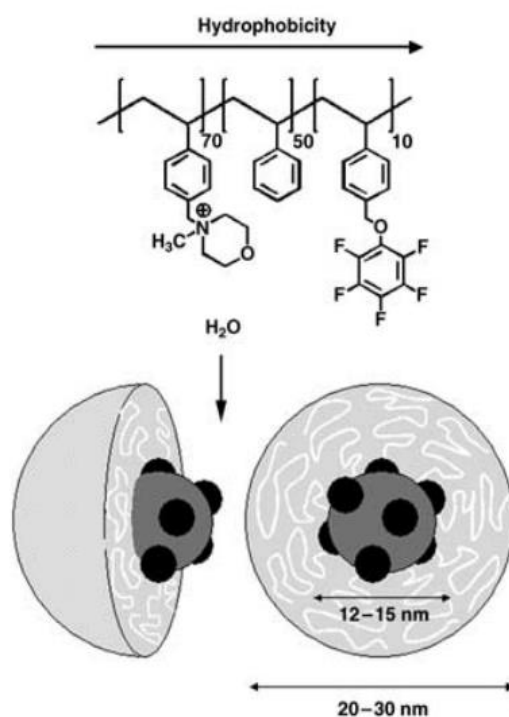

Figure 3. Molecular design and resultant self-assembled multi-compartment micelle
nanostructures, reported in the triphilic triblock copolymer PVBM-*b*-PS-*b*-PVBFP,
adapted with permission from reference 37.

Mecozzi et al. reported the preparation of a novel ABC polymer M2F8H18-based

triphilic Nano emulsion comprising hydrophilic, fluorophilic, and lipophilic interactions

that show long-term stability for up to 1 year.[41] Though a significant number of solution phase self-assembly is reported in the literature, more documentation is needed for bulk-phase self-assembly of ABC linear polymer consisting of these three interactions, as mentioned above. However, a detailed study of resultant self-assembly from such polymers is beneficial, as the incorporation of high χ fluorinated moiety expands the probability of finding well-defined nanostructures by changing the physical properties of the parent molecule.[42] Hillmyer and Lodge suggested that one must incorporate either an ionic moiety or one monomer having high cohesive energy density (CED) and a block with a comparatively lower CED to achieve a high χ in a designed block copolymer. CED measures the polarity and binding energy of each homopolymer block, thus affecting the entire self-assembly. This also reported that perfluorinated alkane monomers could be good candidates since they possess very low CEDs.[42] Incorporating fluorinated and charged blocks in a BCP enhances the possibility of achieving strong interactions at the monomer level that minimizes metastability and increases the degree of segregation gradually. Similarly, the balanced hydrophilic and hydrophobic interactions facilitate the overall χ and ease the formation of a well-defined thermodynamically stable nanostructure. For example, Liu and co-worker showed faster self-assembly to ordered nanoscale areas by their designed triblock copolymer having poly (ether sulfone) and tri-quaternary ammonium functionalized poly (phenylene oxide) as a combination of balanced hydrophobic and hydrophilic interactions.[43] However, the effect on microphase separation of the overall three interactions was not discussed thoroughly. Thus, this work aims to prepare two different triblock copolymer candidates with variable three forces and their effects on self-assembly.

Proposed Designed ABC Block Copolymers with triphilic interactions.

The present work intends to investigate the variable effects of three different interactions (e.g., hydrophobic, hydrophilic, and fluorophilic) in the resultant bulk self-assembly of a triblock terpolymer system. As we anticipate that incorporating all three interactions in the proposed polymers will govern thermodynamically driven self-assembly, this concept was extended to two new unique models of ABC polymers, as shown in **Scheme 1**. Model ABC Polymer **Candidate 1** consists of the hydrophilic moiety poly(lactide) and two hydrophobic moieties, poly(styrene) and poly (hexyl acrylate). Please note that there is no fluorophilic moiety in **Candidate 1**. Whereas **Candidate 2** includes polylactide as a hydrophilic component, polyhexyl acrylate as a hydrophobic/lipophilic, and fluorogenic styrene derivative as a fluorophilic fragment. Another appealing feature of this model is its block sequence, where three different homopolymers are arranged in order of increasing hydrophilicity and making it 'non-frustrated' by preventing the formation of decorated phase with A and C interfaces, such as spheres in lamellae or cylinders on lamellae.[44] As a result, we can assume an increased chance of forming continuous network morphologies.[3]
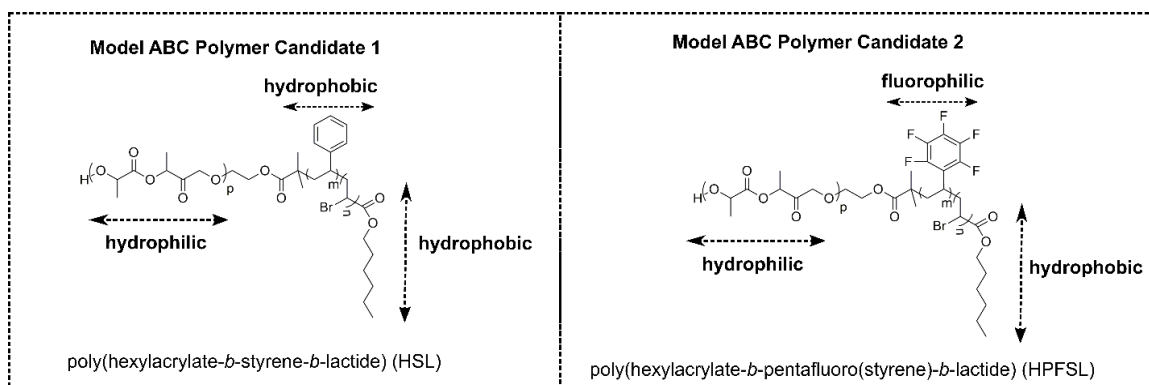
Scheme 1. Molecular architecture of two model ABC polymer candidates having three hydrophobic, hydrophilic, and fluorophilic moieties.

The structure and properties of two ABC model polymer compounds are summarized in **Table 1**. Solubility parameters, including Hansen (HSP) and Hildebrand Solubility Parameters for each block in these proposed polymers, are included in **Table 1**. Hansen Solubility Parameters (HSP) consider the distance between the solvent and the polymer concerning three intermolecular forces, including dispersion (δ_d), polar/dipole-dipole (δ_P), and hydrogen bonding (δ_h) in the Hansen dimension space with the assumption that enthalpic contributions dominate solubilization. Likewise, Hildebrand solubility parameters are estimated based on the cohesive energies of HSP. Thus, the same solubility parameters for a few organic solvents were considered to compare their solubilization ability and choose the best compatible solvent candidate for dissolving the proposed polymers. Analyzing both solubility parameters, we found the best compatible solvents are THF, toluene, chloroform, and polarclean, where both polymer candidates are dissolved and form uniform homogeneous polymer solutions, essential for self-assembly study.

Table 1. Properties of each polymer & proposed solvent candidates.[45-58]

Polymer Candidates & compatible solvents	Homopolymer	Density (gcm^{-3})	Glass Transition Temperature (Tg) °C	Hildebrand Solubility Parameter $(MPa)^{1/2}$	Hansen Solubility Parameter $\delta_D, \delta_P, \delta_H$ $(MPa)^{1/2}$
Candidate 1: HSL	Poly (hexyl acrylate) (PHA)	1.04	-54.15	16.64	----
	Poly (styrene) (PS)	1.05	99.85	18.3	δ_d =5.9 δ_p=18.7 δ_h=3.5
	Poly (lactide) (PLA)	1.26	58.85	20.2 (Krevelen's method) 21.9 (Hoy's method)	δ_d =18.5 δ_P=8 δ_h =7 δ_d =14.2 δ_P=12.73 δ_h =9.77
Candidate 2: HPFSL	Poly (pentafluorostyrene) (PPFS)	1.41	176 170-213.8	0.47*	----
Solvent 1: Tetrahydrofuran (THF)		0.889	----	18.5-19.53	16.8, 5.7, 8.0
Solvent 2: Toluene		0.867	-----	18.2	18.0, 1.4, 2
Solvent 3: Chloroform		1.49	----	19.0	17.8, 3.1, 5.7
Solvent 4: Polar Clean		1.04	----	21.2	15.8, 10.7, 9.2 16.6,13.4, 9.5

---- Data not found/not relevant
* Value obtained from Rajput et.al[57] estimated using Bowden and Jones method.[58]

Experimental Method:

Materials:

Chloroform (>99.8%, ThermoScientific), tetrahydrofuran (THF,

Spectrophotometric grade, 99.7%, ThermoScientific), methanol (>99.9%,

ThermoScientific), Toluene (>99%, extra pure, ThermoScientific), aluminum oxide

(99%, ThermoScientific), styrene (99%, extra pure, stabilized, ThermoScientific),

2,3,4,5,6-pentafluorostyrene (98%, Stab. with 250 ppm 4-tertbutylcatechol,

ThermoScientific), perfluorooctanoic acid (95%, Sigma Aldrich), hexyl acrylate

(stabilized with HQ, 96%, TCI America), benzoic acid (99.5%, Aldrich), 1,8-

Diazabicyclo[5.4.0]undec-7-ene (98%, Aldrich), dimethyl formamide(>99.98%, Fisher),

sodium hydroxide (Fisher), Tris[2-(dimethylamino)ethyl]amine, (97%, Sigma-Aldrich),

copper(I) bromide (99.99% trace metal basis, Sigma Aldrich), tin(II) ethyl hexanoate

(92.5-100%, Millipore sigma), 3,6-Dimethy-1,4-dioxane-2,5-dione (DL Lactide, 99%,

Thermo Scientific), 2-Hydroxyethyl-2-bromoisobutyrate (95%, Sigma Aldrich),

cyclohexylamine (99%, Alfa Aesar), 3,5-bis(trifluoromethylphenyl isothiocyanate) (98%,

Aldrich), and anhydrous chloroform (stabilized with amylene, 99.9%, Across Organics)

were stored in ambient temperature. All reagents were used without further purification

unless otherwise noted.

Characterization:

    NMR Spectroscopy ^{1}H NMR and 19F NMR spectra were collected on a 400

MHz Bruker NMR Spectrometer in $CDCl_3$ at room temperature and analyzed in

MNOVA. ^{1}H NMR chemical shift values (δ) were calibrated using the solvent peak

(from residual solvent protons, 7.26 ppm).

    Gel permeation chromatography (GPC). Synthesized block copolymers were

analyzed by the TOSOH EcoSEC Elite gel permeation chromatography (GPC) system

equipped with TSKgel SuperAWM-H and Super AW2500 column using THF as the

mobile phase (flow rate: 0.35 mL/min, 40 °C). A refractive index (RI) detector for

determining relative length and dispersity. The measurements were carried out on

samples with concentrations of 1 mg/mL that were prepared by stirring at room

temperature overnight and filtered through a 0.22 µm PTFE syringe filter. The number-

average (M_n) and weight-average (M_w) molecular weights, as well as the dispersity (Đ)

were estimated using the polystyrene standards (M_w 589 Da to 8,420 Da).

Small-angle X-ray scattering (SAXS). The X-ray experiments were conducted

using a SAXSLab Ganesha at the South Carolina SAXS Collaborative (SCSC). A Xenocs

GeniX 3D microfocus source was used with a copper target to produce a monochromatic

beam with a 0.154 nm wavelength. The instrument was calibrated before measurements

using the National Institute of Standards and Technology (NIST) silicon reference

material, 640 d, with the peak position at $2\theta = 28.44°$. A Pilatus 300k detector (Dectris)

was used to obtain the 2D scattering patterns with nominal pixel dimensions of 172×172

μm. Transmission small-angle X-ray scattering (SAXS) data were measured. SAXS data

were obtained with an X-ray flux of $\sim$3.3 M photons per second upon the sample and a

detector-to-sample distance of 1040 mm. The 2D images were azimuthally integrated to

yield the scattering vector and intensity.

Thermogravimetric Analysis. Thermal analyses of the synthesized polymers

were performed with a Differential Scanning Calorimeter TA Instrument Discovery DSC

in a temperature range of -75 to 250 ℃ at a heating rate of 10 ℃ min^{-1} under a nitrogen

flow of 60 mL min^{-1}. The glass transition temperature (T_g) was determined from the

second heating trace and is reported as the midpoint of the thermal transition. Thermal

degradation of the synthesized polymers was investigated by thermogravimetric analysis

(TGA) performed with a TA Instruments Discovery TGA. Measurements were conducted

from 25 to 500 ℃ at a rate of 10 ℃ min^{-1} in a nitrogen flow of 60 mL min^{-1}.
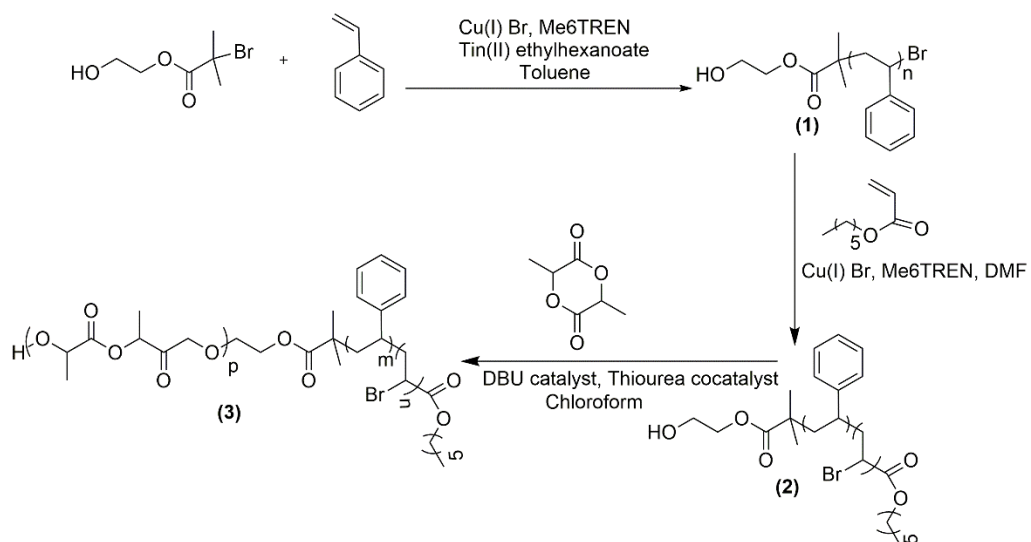
Scheme 2. Polymer **Candidate 1 HSL (3)** Synthesis steps.

Synthesis of Model Polymer Candidate 1 HSL (shown in Scheme 2):

1. Synthesis of hydroxyl-terminated polystyrene (PS-OH) macroinitiator **(1)**.

The **PS-OH** macroinitiator was synthesized *via* ARGET-ATRP using a reagent ratio of

[styrene] : [2-hydroxy ethyl bromoisobutyrate] : [Me$_6$TREN] : [Cu(I)] : [Sn (II)] = 300 : 1

 : 0.105 : 0.005 : 0.1. At first the monomer styrene was passed through the alumina

column to remove the inhibitor. To a Schlenk flask, 110 mL of inhibitor-free styrene (960

mmol) and 464 µL of 2-hydroxy-2-ethyl bromoisobutyrate (3.2 mmol) were added. The

flask was sparged with nitrogen (N$_2$) gas for 15 minutes. A catalyst stock solution of 0.5

mL of toluene containing 3 mg of Cu(I)Br (0.016 mmol), 90 µL (0.336 mmol) of

Me$_6$TREN ligand, and 104 µL of Sn (II) ethyl hexanoate (0.320 mmol) was added to the

reaction flask under flowing N$_2$ gas. This reaction mixture was then placed into a

preheated oil bath at 90 °C with constant stirring. The polymerization continued for 26 h,

and the reaction mixture was cooled with ice water at the end before exposing the

solution to air. The crude polymerization solution was diluted with THF and precipitated two times into 10-fold excess of cold methanol. The product was filtered and vacuum dried at 40 °C for 48 h. The number average molecular weight (M_n) and molar mass dispersity $Đ$ = were determined using ^{1}H NMR and a PS-calibrated GPC, presented in **Table 2**.

2. *Synthesis of poly (styrene-block-hexyl acrylate) (HS) diblock copolymer* (**2**). The **HS** macroinitiator was synthesized *via* ATRP using a reagent ratio of [HA] : [PS] : [Me$_6$TREN] : [Cu(I)] = 100 : 1 : 0.5 : 0.5. To a Schlenk flask, a 10 g PS macroinitiator was dissolved in 100 mL DMF. After complete dissolution, 25 mL of inhibitor-free HA monomer (139 mmol) was added to it. The flask was degassed and backfilled with nitrogen (N$_2$) gas. A catalyst solution of 1 mL of toluene containing 100 mg of Cu(I)Br (0.694 mmol) and 160 μL (0.694 mmol) of Me$_6$TREN ligand was added to the reaction flask under flowing N$_2$ gas. This reaction mixture was then placed into a preheated oil bath at 70 °C with constant stirring. The polymerization was continued for 96 h, and the reaction mixture was cooled with ice water at the end before exposing the solution to air. The crude polymerization solution was diluted with DMF, passed through the alumina column to remove trace amounts of Cu, and precipitated two times into 10-fold excess of cold methanol. The product was filtered and vacuum dried at 40 °C for 48 h. The number average molecular weight (M_n) and molar mass dispersity $Đ$ = were determined using ^{1}H NMR and a PS-calibrated GPC, presented in **Table 2.**

3. *Synthesis of HSL triblock terpolymer* (**3**). The **SH** macroinitiator was chain extended from the terminal hydroxyl group via organocatalytic ring-opening polymerization (ROP) using a reagent ratio of [SH]: [lactide]: [DBU]: [thiourea] =

1:80:1.34:1.34. Before starting the reaction, the **SH** macroinitiator and D, L-lactide

monomer were each dried separately overnight at 40 °C under a high vacuum before

being transferred to a sealed Schlenk flask. The **SH** (1 g, 0.055 mmol) and lactide

monomer (600 mg) were combined with thiourea co-catalyst (27 mg, 0.074 mmol). All

the reagents were dissolved in 10 mL of anhydrous chloroform. After dissolution, the

DBU catalyst (11 µL, 0.074 mmol) was added to the polymerization mixture dropwise,

and the reaction was stirred at RT for 30 min. The reaction was terminated by adding

benzoic acid (9 mg, 0.074 mmol). The polymer solution was precipitated twice into 10-

fold excess of cold methanol. The product was filtered and vacuum dried at 40 °C for 48

h. The number average molecular weight (M_n) and molar mass dispersity $Đ =$ were

determined using ^{1}H NMR and a PS-calibrated GPC.
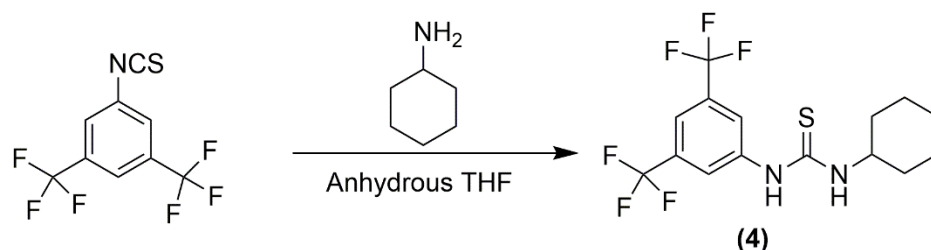
Scheme 3. Synthesis of co-catalyst bis(3,5-trifluoromethyl) phenyl cyclohexyl thiourea

(4).

Synthesis of co-catalyst bis(3,5-trifluoromethyl) phenyl cyclohexyl thiourea (shown

in Scheme 3):

The ROP co-catalyst (**4**) was synthesized following a reported procedure.[59] The

synthesis was performed in a sealed Schlenk flask where 3,5-bis(trifluoromethyl)

phenylisothiocyanate (3.37 mL, 18.5 mmol) and anhydrous THF (20 mL) were combined

in a round bottom flask that was previously dried using a heat-gun and contained a

magnetic stir bar. In the glovebox, cyclohexylamine (2.11 mL, 18.5 mmol) was added to

the stirring solution dropwise via a syringe. The reaction continued at room temperature

for 24 h, and THF was removed using a rotary evaporator. The white residue was

recrystallized twice from chloroform and stored after drying under a vacuum at 40 °C for

48. The product was characterized by ^{1}H NMR.
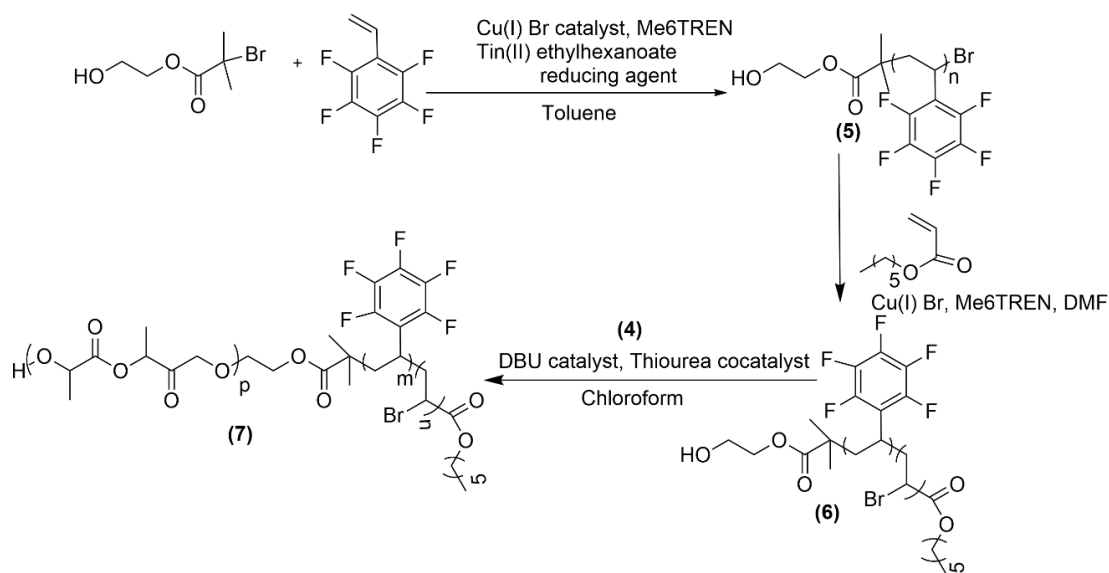
Scheme 4. Polymer **Candidate 2 HPFSL (7)** Synthesis steps.

Synthesis of Model Polymer Candidate 2 HPFSL (shown in Scheme 4):

    1. Synthesis of hydroxyl-terminated poly pentafluorostyrene (PFS-OH)

macroinitiator **(5)**. The **PFS-OH** macroinitiator was synthesized *via* ARGET-ATRP

using a reagent ratio of [pentafluorostyrene] : [2-hydroxy ethyl bromoisobutyrate] :

[Me$_6$TREN] : [Cu(I)] : [Sn (II)] = 120 : 1 : 0.105 : 0.005 : 0.1. At first the monomer

pentafluorostyrene was passed through the alumina column to remove the inhibitor. To a

Schlenk flask, 35 mL of inhibitor-free pentafluorostyrene (258 mmol), 35 mL toluene,

and 311 μL of 2-hydroxy-2-ethyl bromoisobutyrate (2.15 mmol) were added. The flask

was sparged with nitrogen (N$_2$) gas for 15 minutes. A catalyst stock solution of 0.5 mL of

toluene containing 2 mg of Cu(I)Br (0.0107 mmol), 60 µL (0.225 mmol) of Me_6TREN

ligand, and 70 µL of Sn (II) ethylhexanoate (0.215 mmol) was added to the reaction flask

under flowing N_2 gas. This reaction mixture was then placed into a preheated oil bath at

90 °C with constant stirring. The polymerization continued for 49 h, and the reaction

mixture was cooled with ice water before exposing the solution to air. The crude

polymerization solution was diluted with THF and precipitated two times into 10-fold

excess of cold methanol. The product was filtered and vacuum dried at 40 °C for 48 h.

The number of average molecular weight (M_n) and molar mass dispersity $Đ$ = was

determined using ^{1}H NMR and a PS-calibrated GPC, presented in **Table 2.**

2. Synthesis of poly (pentafluorostyrene-block-hexyl acrylate) **(PFSH)** *diblock*

copolymer (**6**).

The **PFSH** macroinitiator was synthesized *via* ATRP using a reagent ratio of [HA] :

[PFSH] : [Me_6TREN] : [Cu(I)] = 50 : 1 : 0.5 : 0.5. To a Schlenk flask, a 10 g PS

macroinitiator was dissolved in 30 mL DMF. After complete dissolution, 17 mL of

inhibitor-free HA monomer (94 mmol) was added to it. The flask was degassed and

backfilled with nitrogen (N_2) gas. A catalyst solution of 2 mL of toluene containing 135

mg of Cu(I)Br (0.943 mmol) and 217 µL (0.943 mmol) of Me_6TREN ligand was added to

the reaction flask under flowing N_2 gas. This reaction mixture was then placed into a

preheated oil bath at 70 °C with constant stirring. The polymerization continued for 48 h,

and the reaction mixture was cooled with ice water before exposing the solution to air.

The crude polymerization solution was diluted with DMF, passed through the alumina

column to remove trace amounts of Cu, and precipitated two times into 10-fold excess of

cold methanol. The product was filtered and vacuum dried at 40 °C for 48 h. The number

average molecular weight (M_n) and molar mass dispersity $Đ =$ were determined using [1]H

NMR and a PS-calibrated GPC, presented in **Table 2.**

      3. Synthesis of PFSHL triblock terpolymer (**7**)*.* The **PFSH** macroinitiator was

chain extended from the terminal hydroxyl group via organocatalytic ring-opening

polymerization (ROP) using a reagent ratio of [SH]: [lactide]: [DBU]: [thiourea] =

1:50:1.34:1.34. Before starting the reaction, the **PFSH** macroinitiator and D, L-lactide

monomer were each dried separately overnight at 40 °C under a high vacuum before

being transferred to a sealed Schlenk flask. The **PFSH** (1 g, 0.154 mmol) and lactide

monomer (1.1 g, 7.71 mmol) were combined with thiourea co-catalyst (74 mg, 0.207

mmol). All the reagents were dissolved in 10 mL of anhydrous chloroform. After

dissolution, the DBU catalyst (31 μL, 0.207 mmol) was added to the polymerization

mixture dropwise, and the reaction was stirred at RT for 60 min. The response was

terminated by adding benzoic acid (25 mg, 0.207 mmol). The polymer solution was

precipitated twice into 10-fold excess of cold methanol. The product was filtered and

vacuum dried at 40 °C for 48 h. The number average molecular weight (M_n) and molar

mass dispersity $Đ =$ were determined using ^{1}H NMR and a PS-calibrated GPC**.**

Solubility and Polymer Bulk Film Preparation

      Both **HSL7** and **HPFSL4** displayed good solubility in THF, toluene, chloroform,

and PolarClean, as the solubility values of the corresponding solvents match with the

representative homopolymer (**Table 1**). For example, 10 wt %

THF/toluene/chloroform/polarclean solutions of **HSL7** and **HPFLS4** can be prepared

readily. Uniform polymer bulk films up to ~0.5 mm in thickness were easily obtained by

drop casting followed by thermal annealing, which suggests the good processability of the synthesized polymers.

Result & Discussion:

   Polymer Synthesis & Characterization: This thesis presents a facile pathway to fabricate large-scale polymers with well-defined macromolecular architecture and tunable hydrophobic, hydrophilic, and fluorophilic interactions, combining controlled and "living" polymerization approaches such as Atom Transfer Radical Polymerization (ATRP), Activator Regenerated Atom Transfer Radical Polymerization (ARGET-ATRP) and Ring-Opening Polymerization (ROP). Synthetic strategies to obtain designed model ABC polymer candidates are presented in **Scheme 2** and **Scheme 4**. **Scheme 2** illustrates the synthesis of **Candidate 1**, poly (hexyl acrylate)-*b*-polystyrene-*b*-polylactide (**HSL, 3**), where the first step was the synthesis of bi-functional macroinitiator poly(styrene) (PS) via Activator Regenerated Electron Transfer-Atom Transfer Radical Polymerization (ARGET-ATRP).[60] Polymerization was initiated with a 2-hydroxyethyl Bromo isobutyrate initiator and styrene monomer in the presence of Cu(I) catalyst and Sn (II) ethyl hexanoate reducing agent. ARGET-ATRP was preferred over ATRP for the synthesis of polystyrene because, in an ATRP process, the concentrations of radicals are relatively lower, which is not ideal for preparing well-defined materials.   In addition, the higher amount of copper catalyst used in ATRP allows for side reactions to occur mainly through outer sphere electron transfer (OSET), where the radical is oxidized in the presence of deactivator Cu^{+2} or reduced in the presence of Cu^{+1}. In contrast, in ARGET-ATRP, only a few ppm amounts of a very active copper catalyst are necessary to initiate the reaction. Jakubowski et al. mention that the synthesis of polystyrene via ATRP is

subject to the β-Hydride elimination reaction induced by the Cu^{+2} deactivator causing the highest contribution to the loss of end-chain functionality. The authors demonstrated the synthesis of polystyrene by ARGET-ATRP with 92% monomer conversion, whereas ATRP reported only 48%. Along with control over molecular weight and narrow dispersity provided by ATRP, ARGET-ATRP improves end-chain functionality and reduces the amount of waste by using lower amounts of copper catalyst for the synthesis of polystyrene. [60] In the second step, the hexyl acrylate chain was extended by ATRP reaction to form polystyrene-b-poly hexyl acrylate (**SH**) diblock copolymer. The rate of the solution polymerization depends on the reaction condition; for example, around ~25% monomer conversion was obtained for **SH** with the [100]:[1] ([monomer HA]: [PS macroinitiator)] ratio when the reaction was continued for 24 hours at 70 ℃. This conversion gets higher up to 67% when the same response was continued for 96 hours at the same condition. $CuBr/Me_6TREN$ catalyst/ligand complex was used to enhance the initiation rate over propagation. At the very last step, the HSL triblock copolymer was synthesized by reacting the SH terminal- OH group with DL lactide in the presence of catalyst DBU and thiourea cocatalyst (the synthesis procedure is described in **Scheme 3**). Synthesis was performed at room temperature, anhydrous chloroform media under a nitrogen environment to avoid transesterification,[61] and we obtained a high degree of control in hydrophilic block insertion in the resultant polymer via this approach. The synthesized HSL polymer was characterized by ^{1}H NMR; a characterization of ^{1}H NMR data for a representative polymer **HSL6** is shown in **Figure 4**. The ^{1}H NMR spectrum shows the incorporation of each homopolymer, such as peaks at δ6.3-7.2 ppm for aromatic protons for PS, δ2.3 and δ4.0 ppm for PHA, and δ5.2 ppm for PLA proton

peaks, respectively. This synthesis procedure generated a series of HSL triblock

copolymers with varying hydrophilic to hydrophobic contents, shown in **Table 2**.

Likewise, polymer **Candidate 2 HPFLS** was synthesized following a similar procedure,

while the monomers were changed to styrene derivative 2,3,4,5,6-pentafluorostyrene.

Stepwise synthesis details for **HPFSL** are laid out in **Scheme 4** and characterized using

multinuclear NMR spectroscopy. The 1H NMR (Figure 5) for HPFSL is collectively

similar to the **HSL**, except the aromatic protons are missing in the former NMR profile as

F atoms in pentafluoro styrene monomer replace all the aromatic protons. Additional ^{19}F

NMR (**Figure 6**) signals for **HPFSL** were observed at -143, -154, and -161 ppm, which

were attributed to the ortho-, para- and meta-F groups in the pentafluoro styrene side

chain, respectively. Though molecular weights of these polymers were estimated based

on the end-group analysis of ^{1}H NMR spectroscopy, gel permeation chromatography

(GPC) was used further to assess the molecular weights and dispersity of the resultant

polymer materials. The facile synthetic approach enables the synthesis of both polymers
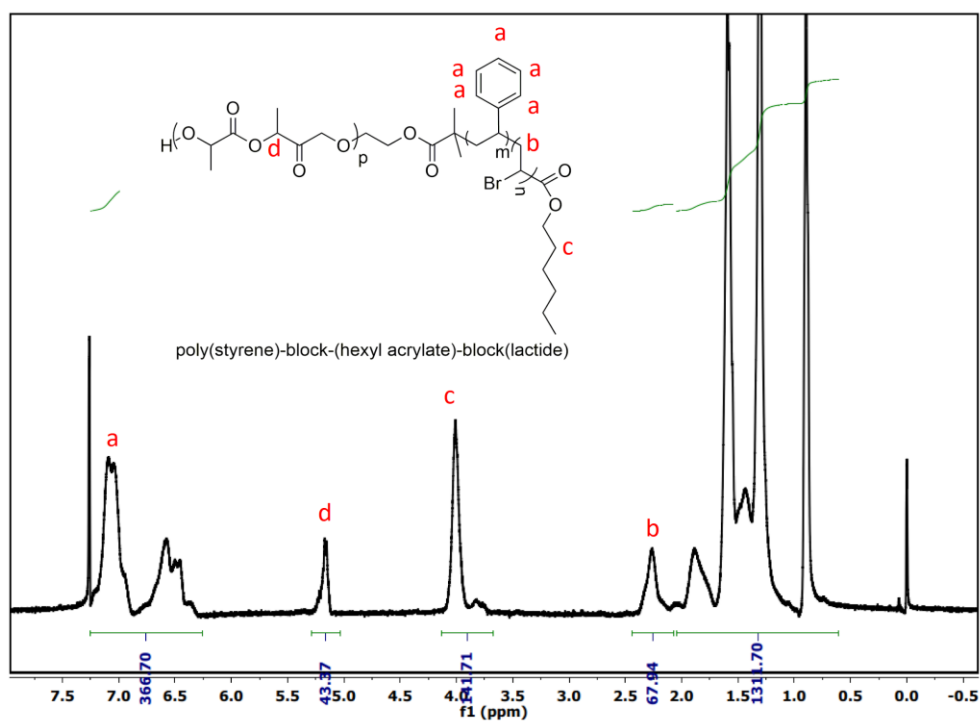
on a large scale (e.g., 20 g).

Figure 4. ^{1}H NMR of Polymer **Candidate 1 HSL6,** end-group analysis suggests the M$_n$ is 24.3 kg/mol, shown in **Table 2**.
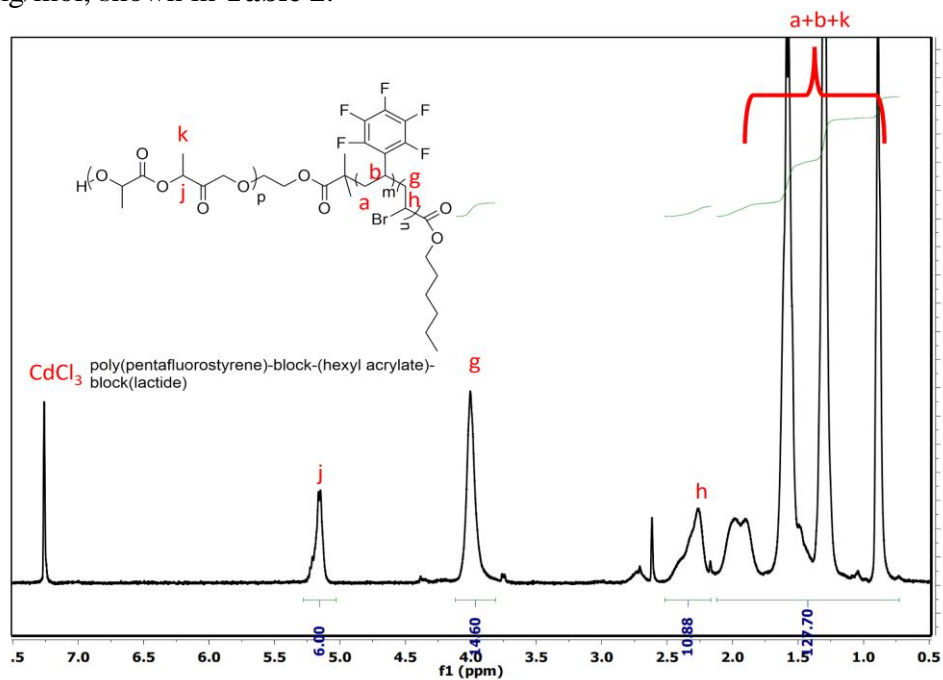

Figure 5. ^{1}H NMR of Polymer **Candidate 2 HPFLS4,** end-group analysis suggests the M$_n$ is 9.5 kg/mol, shown in **Table 2**.
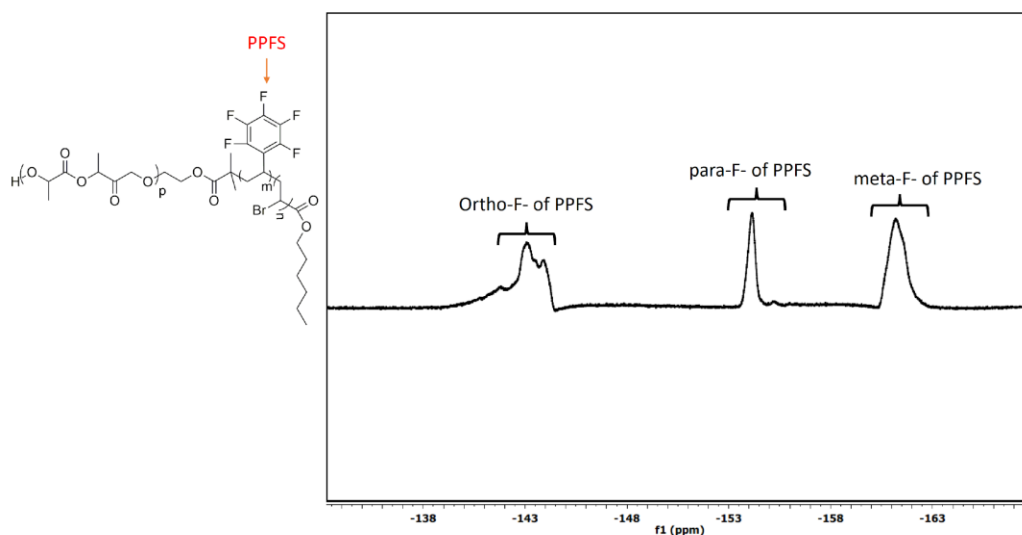
Figure 6. ^{19}F NMR of Polymer **Candidate 2 HPFLS4** demonstrates the successful incorporation of fluorogenic moiety in the synthesized polymer.

Table 2. Characterization of the synthesized ABC model polymer candidates

| Polymer	M_n, NMR kg/mol	M_n, GPC kg/mol	M_w, GPC kg/mol	Đ	%W_f, styrene derivative	%W_f, acrylate derivative	%W_f, lactide	Tunability of forces
HSL1	13.5				54	32	14	Hydrophobic force dominates, and no fluorophilic force.
HSL5	14.3				50	34	15	Hydrophobic force dominates, and no fluorophilic force.
HSL6	24.3				31	43	25	Hydrophobic force dominates, and no fluorophilic force.
HSL7	19.7	38.8	47.8	1.23	39	53	8	Hydrophobic force dominates, and no fluorophilic force.
HSL9	36.5				21	26	53	Hydrophilic force dominates, no fluorophilic force.
HSL10	82	43.1	58.6	1.36	9	14	77	Hydrophilic force dominates, no fluorophilic force.
HPFSL1	7.3				72	16	12	Fluorophilic>Hydrophobic>Hydrophilic
HPFSL4	9.5	39.1	51.6	1.32	56	12	32	Fluorophilic>Hydrophilic>Hydrophobic

Here H = Poly (hexyl acrylate), S = Polystyrene, L= Poly(lactide), PFS= poly(pentafluorostyrene)
1-10 is the synthesis batch number.

GPC data (**Figure 4** and **Figure 5**) for both polymer candidates showed marked shifts to the lower retention time or higher molecular weights upon chain extension and ring-opening polymerization that finally led to a successful synthesis of ABC triblock copolymer. The M_n for all ABC polymers determined by GPC was higher than that determined by ^{1}H NMR. This difference could be attributed to the M_n determined by GPC typically calculated relative to the calibration agent PS. Additionally, the hydrodynamic volumes of the other two homopolymers, PHA and PLA, are very different from PS, which might result in differences in calculated and actual molecular weights.[62] In a few cases, bimodal molecular weight distributions were observed (such as HPFSL**4)** with a higher dispersity value (Đ>1.4) which is most likely due to an improper chain coupling reaction that is quite common in radical polymerization and ring opening polymerization reactions, especially during the synthesis of high molecular weights polymer. Overall, all these data confirm the successful synthesis of the proposed ABC polymer candidates, successfully tuning the different ratios of hydrophilic, hydrophobic, and fluorophilic interactions. Detailed structural characteristics for all the synthesized polymers are summarized in **Figure 7**, **Figure 8,** and **Table 2.**
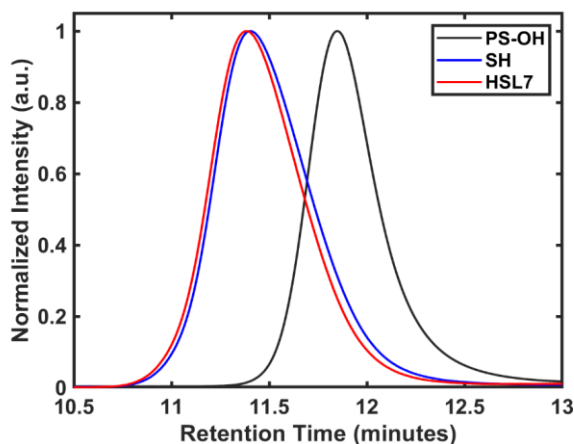
Polymer Block	M_n (K gmol^{-1})	M_w (K gmol^{-1})	Dispersity (Đ)
PS-OH	16.3	19.4	1.19
SH	35.9	45.1	1.25
HSL7	38.8	47.8	1.23

Figure 7. GPC trace of each block polystyrene macroinitiator (**PS-OH**), **SH** diblock copolymer, and Polymer **Candidate 1 HSL7.** Each block M_n, M_w, and dispersity (Đ) are listed above**.**
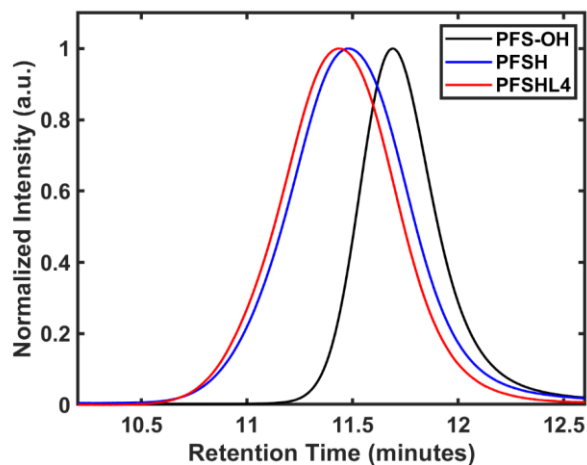
Polymer Block	M_n (K gmol^{-1})	M_w (K gmol^{-1})	Dispersity (Đ)
PFS-OH	22.9	26.9	1.18
PFSH	34.8	47.2	1.35
PFSHL4	39.1	51.6	1.32

Figure 8. GPC trace of each block polystyrene macroinitiator (**PFS-OH**), **PFSH** diblock copolymer, and Polymer **Candidate 2 PFSHL4.** Each block M_n, M_w, and dispersity (Đ) are listed above**.**

**Thermal Stability of the Synthesized Polymer Candidates**:

Thermal stabilities of these synthesized polymers were determined by TGA; the resulting TGA profile is shown in **Figure 9,** along with the extracted data. As seen, both polymers demonstrate similar high thermal stability. Thermal degradation temperatures for **HSL7** and **HPFSL4** were noted at ~400 ºC for ~50% decomposition. Please note that the M_n of **HFSL4** is lower than **HSL7**, as suggested by ^{1}H NMR end-group analysis (**Table 2**). Thus, we concluded that the incorporation of F moiety as a substituent in the styrene did improve the thermal stability of lower molecular weight **HPFSL4**.[63]. Likewise, the glass transition temperature (Tg) of each contributing homopolymer in both polymers was estimated based on their DSC profile (**Figure 10**). The PHA, PS/PFS, and PLA homopolymers demonstrated the Tgs' in the range of -47 to -53, 33 to 34, and 109 ºC, respectively.
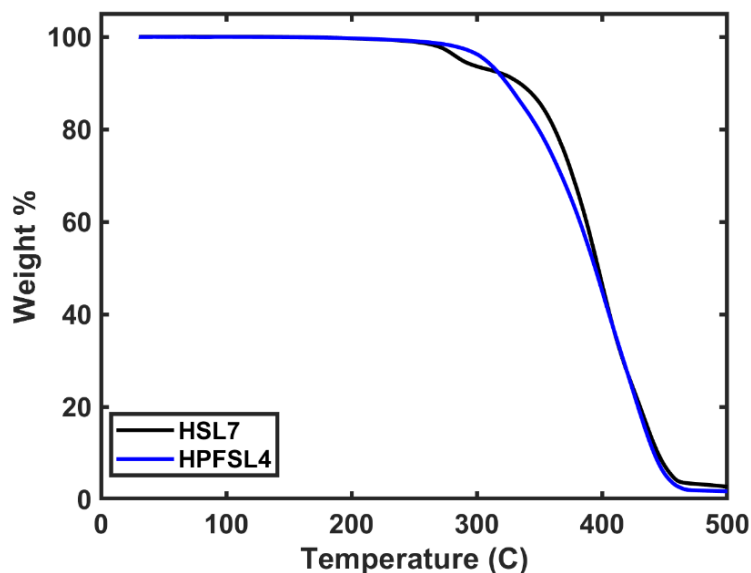
Polymers	T_{dec1} (ºC)	T_{dec2} (ºC)
HSL7	396.2	445.1
HPFSL4	395.4	445.2

Figure 9. Thermal stability of **HSL7** and **HPFSL4**, measured by TGA. T_{dec1} & T_{dec2} values represent the temperatures at which 50% and 90% of the weights are lost, respectively.
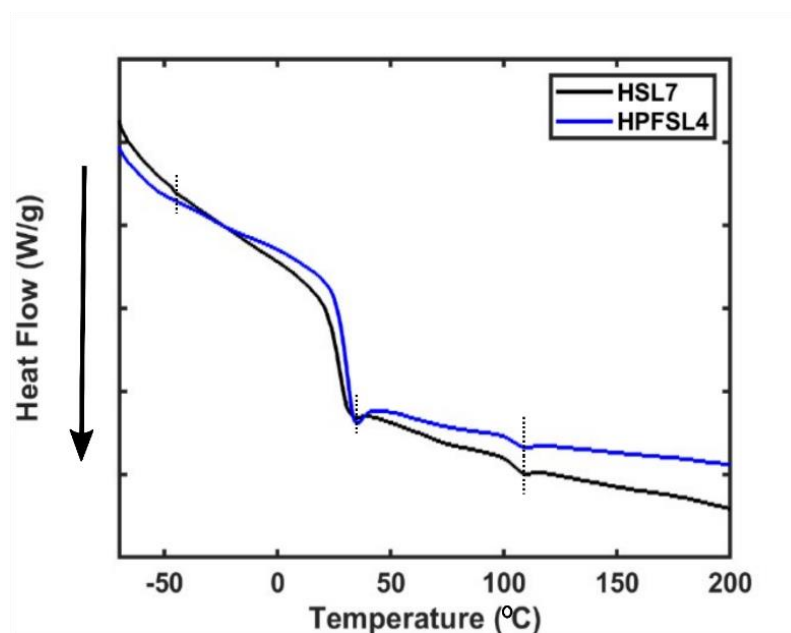
Polymers	Homopolymers	T_g (ºC)
HSL7	PS	108.9
	PHA	-46.7
	PLA	32.8
HPFSL4	PFS	108.9
	PHA	-53.0
	PLA	34.2

Figure 10. Comparison of DSC curves (exo down) of **HSL7** and **HPFSL4** block copolymers. The glass transition temperatures (T_g) of each homopolymer are shown by dotted lines and listed in the above table.

Bulk Self-Assembly

Small-angle X-ray scattering (SAXS) was employed on the polymer candidates'

solid free-standing films to obtain the bulk morphology and domain dimensions (**Figure**

11). Diffraction peaks occur at integer multiples of the principle wavevector q*,

suggesting lamellar morphologies for **HPFSL4**. In comparison, only one peak for **HSL7**

indicated a state of disorder or lack of long-range ordering. This data clearly showed that

incorporating Fluorine moiety in the resultant polymer **HPFSL4** enables a balance of

hydrophilic, hydrophobic, and fluorophilic interactions, thus increasing the overall χ and

easing the attainment of thermodynamically driven LAM morphology. At the same time,

the absence of this combination of triphilic interaction causes the poorly ordered

nanostructure formation in the comparable polymer **HSL7**.
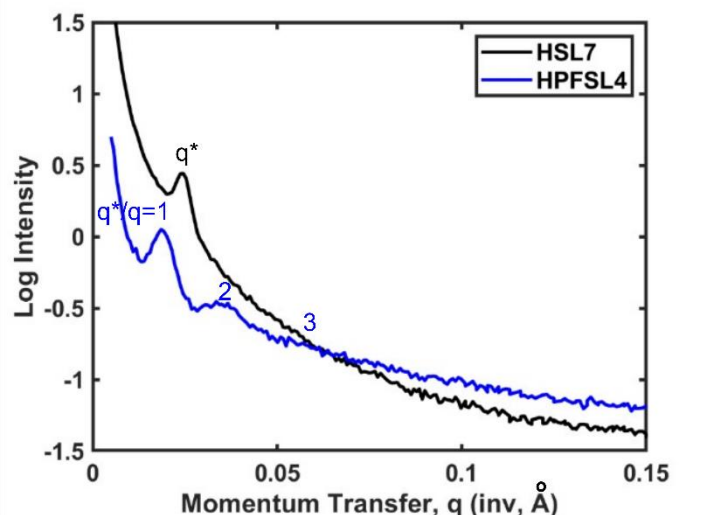
Polymers	d-spacing (nm)	q/q* ratio	Suggested nanoscale morphology
HSL7	26.5	--	Disordered/poorly ordered (DIS)
HPFSL4	35.5	1:2:3	Lamellar (LAM)

Figure 11. SAXS of HSL7 and HPFSL4 bulk polymer films. The samples were indexed
for LAM symmetry with peaks indicated at q/q*=1, 2, 3, 4, and 5. The scattering data
were offset vertically for clarity.

Conclusion & Future Work

This current work validates a design for two novel ABC triblock copolymers via controlled radical and organocatalytic ring-opening polymerization. The resultant polymer demonstrated thermal stability up to 400 ºC and showed thermodynamically driven self-assembly phenomena. We achieved the right balance of hydrophilic, hydrophobic, and fluorophilic interactions synthetically by tuning the variable fluorinated linker in the resultant polymers. In the future, this work will be extended to other ABC polymer varying fluorinated linkers that may offer more advanced and exotic nanostructures compared to traditional ABC polymer. Future work would be concentrated on investigating these synthesized polymers' roles as a sorbent for poly and perfluoroalkyl substances (PFAS) from drinking water. We expect to gain a mechanistic understanding of interfacial phenomena in successfully removing PFAS. Both polymers were synthesized on a mass scale with no additional post-synthetic transformation and tedious monomer synthesis that eventually would influence their commercial viability.

References

1. Thomas, Edwin L., et al. "Periodic Area-Minimizing Surfaces in Block Copolymers." *Nature*, vol. 334, no. 6183, 18 Aug. 1988, pp. 598–601., https://doi.org/10.1038/334598a0.

2. Bates, Frank S. "Polymer-Polymer Phase Behavior." *Science*, vol. 251, no. 4996, 22 Feb. 1991, pp. 898–905., https://doi.org/10.1126/science.251.4996.898.

3. Bates, Frank S., and Glenn H. Fredrickson. "Block Copolymers—Designer Soft Materials." *Physics Today*, vol. 52, no. 2, 1999, pp. 32–38., https://doi.org/10.1063/1.882522.

4. Zhang, Lifeng, and Adi Eisenberg. "Multiple Morphologies of 'Crew-Cut' Aggregates of Polystyrene- *b* -Poly (Acrylic Acid) Block Copolymers." *Science*, vol. 268, no. 5218, 1995, pp. 1728–1731., https://doi.org/10.1126/science.268.5218.1728.

5. Zhang, Lifeng, et al. "Ion-Induced Morphological Changes in 'Crew-Cut' Aggregates of Amphiphilic Block Copolymers." *Science*, vol. 272, no. 5269, 1996, pp. 1777–1779., https://doi.org/10.1126/science.272.5269.1777.

6. Bates, Frank S., and Glenn H. Fredrickson. "Block Copolymer Thermodynamics: Theory and Experiment." *Annual Review of Physical Chemistry*, vol. 41, no. 1, 1990, pp. 525–557., https://doi.org/10.1146/annurev.pc.41.100190.002521.

7. Matsen, M. W., and F. S. Bates. "Unifying Weak- and Strong-Segregation Block Copolymer Theories." *Macromolecules*, vol. 29, no. 4, 1996, pp. 1091–1098., https://doi.org/10.1021/ma951138i.

8. Matsen, M. W., and M. Schick. "Stable and Unstable Phases of a Diblock Copolymer Melt." *Physical Review Letters*, vol. 72, no. 16, 1994, pp. 2660–2663., https://doi.org/10.1103/physrevlett.72.2660.

9. Abetz, Volker, and Reimund Stadler. "ABC and BAC Triblock Copolymers - Morphological Engineering by Variation of the Block Sequence." *Macromolecular Symposia*, vol. 113, no. 1, 1997, pp. 19–26., https://doi.org/10.1002/masy.19971130105.

10. Zheng, Wei, and Zhen-Gang Wang. "Morphology of ABC Triblock Copolymers." *Macromolecules*, vol. 28, no. 21, 1995, pp. 7215–7223., https://doi.org/10.1021/ma00125a026.

11. Mogi, Yasuhiro, et al. "Preparation and Morphology of Triblock Copolymers of the ABC Type." *Macromolecules*, vol. 25, no. 20, 1992, pp. 5408–5411., https://doi.org/10.1021/ma00046a043.

12. Mogi, Yasuhiro, et al. "Superlattice Structures in Morphologies of the ABC Triblock Copolymers." *Macromolecules*, vol. 27, no. 23, 1994, pp. 6755–6760., https://doi.org/10.1021/ma00101a013.

13. Matsushita, Yushu, et al. "Surfaces of Tricontinuous Structure Formed by an ABC Triblock Copolymer in Bulk." *Physica B: Condensed Matter*, vol. 248, no. 1-4, 1998, pp. 238–242., https://doi.org/10.1016/s0921-4526(98)00239-7.

14. Bailey, Travis S., et al. "A Noncubic Triply Periodic Network Morphology in Poly (Isoprene-*b*-Styrene-*b*-Ethylene Oxide) Triblock Copolymers." *Macromolecules*, vol. 35, no. 18, 2002, pp. 7007–7017., https://doi.org/10.1021/ma011716x.

15. Epps, Thomas H., et al. "Ordered Network Phases in Linear Poly (Isoprene-*b*-Styrene-*b*-Ethylene Oxide) Triblock Copolymers." *Macromolecules*, vol. 37, no. 22, 2004, pp. 8325–8341., https://doi.org/10.1021/ma048762s.

16. Tyler, Christopher A., and David C. Morse. "Orthorhombic F d d d Network in Triblock and Diblock Copolymer Melts." *Physical Review Letters*, vol. 94, no. 20, 2005, https://doi.org/10.1103/physrevlett.94.208302.

17. Goldacker, Thorsten, et al. "Non-Centrosymmetric Superlattices in Block Copolymer Blends." *Nature*, vol. 398, no. 6723, 1999, pp. 137–139., https://doi.org/10.1038/18191.

18. Li, Zhibo, et al. "Multicompartment Micelles from ABC Miktoarm Stars in Water." *Science*, vol. 306, no. 5693, 2004, pp. 98–101., https://doi.org/10.1126/science.1103350.

19. Krappe, Udo, et al. "Chiral Assembly in Amorphous ABC Triblock Copolymers. Formation of a Helical Morphology in Polystyrene-Block-Polybutadiene-Block-Poly (Methyl Methacrylate) Block Copolymers." *Macromolecules*, vol. 28, no. 13, 1995, pp. 4558–4561., https://doi.org/10.1021/ma00117a027.

20. Kaneko, Takeshi, et al. "A 'Ladder' Morphology in an ABC Triblock Copolymer." *Macromolecular Symposia*, vol. 242, no. 1, 2006, pp. 80–86., https://doi.org/10.1002/masy.200651013.

21. Park, Cheolmin, et al. "Enabling Nanotechnology with Self Assembled Block Copolymer Patterns." *Polymer*, vol. 44, no. 22, 2003, pp. 6725–6760., https://doi.org/10.1016/j.polymer.2003.08.011.

22. Chang, Alice B., and Frank S. Bates. "The Abcs of Block Polymers." *Macromolecules*, vol. 53, no. 8, 2020, pp. 2765–2768., https://doi.org/10.1021/acs.macromol.0c00174.

23. Li, Zhibo, et al. "Morphologies of Multicompartment Micelles Formed by ABC Miktoarm Star Terpolymers." *Langmuir*, vol. 22, no. 22, 2006, pp. 9409–9417., https://doi.org/10.1021/la0620051.

24. Zhou, Zhilian, et al. "Micellar Shape Change and Internal Segregation Induced by Chemical Modification of a Tryptych Block Copolymer Surfactant." *Journal of the American Chemical Society*, vol. 125, no. 34, 2003, pp. 10182–10183., https://doi.org/10.1021/ja036551h.

25. Thünemann, Andreas F., et al. "Two-Compartment Micellar Assemblies Obtained via Aqueous Self-Organization of Synthetic Polymer Building Blocks." *Langmuir*, vol. 22, no. 6, 2006, pp. 2506–2510., https://doi.org/10.1021/la0533720.

26. Weberskirch, R., et al. "Design and Synthesis of a Two Compartment Micellar System Based on the Self-Association Behavior of Poly(n-Acylethyleneimine) End-Capped with a Fluorocarbon and a Hydrocarbon Chain." *Macromolecular Chemistry and Physics*, vol. 201, no. 10, 2000, pp. 995–1007., https://doi.org/10.1002/1521-3935(20000601)201:10<995::aid-macp995>3.0.co;2-t.

27. Kubowicz, Stephan, et al. ``Cylindrical Micelles of α-Fluorocarbon-ω-Hydrocarbon End-Capped Poly(*n*-Acylethylene Imine)s." *Langmuir*, vol. 21, no. 16, 2005, pp. 7214–7219., https://doi.org/10.1021/la050987o.

28. Mao, Jiang, et al. "Multicompartment Micelles from Hyperbranched Star-Block Copolymers Containing Polycations and Fluoropolymer Segment." *Langmuir*, vol. 23, no. 9, 2007, pp. 5127–5134., https://doi.org/10.1021/la063576w.

29. Lodge, Timothy P., et al. "Access to the Superstrong Segregation Regime with Nonionic ABC Copolymers." *Macromolecules*, vol. 37, no. 18, 2004, pp. 6680–6682., https://doi.org/10.1021/ma048708b.

30. Lodge, Timothy P., et al. "Simultaneous, Segregated Storage of Two Agents in a Multicompartment Micelle." *Journal of the American Chemical Society*, vol. 127, no. 50, 2005, pp. 17608–17609., https://doi.org/10.1021/ja056841t.

31. Kubowicz, Stephan, et al. "Multicompartment Micelles Formed by Self-Assembly of Linear ABC Triblock Copolymers in Aqueous Medium." *Angewandte Chemie International Edition*, vol. 44, no. 33, 2005, pp. 5262–5265., https://doi.org/10.1002/anie.200500584.

32. Skrabania, Katja, et al. "Synthesis and Micelar Self-Assembly of Ternary Hydrophilic-Lipophilic-Fluorophilic Block Copolymers with a Linear PEO Chain. *Langmuir*, vol. 25, no. 13, 2009, pp. 7594–7601., https://doi.org/10.1021/la900253j.

33. Berlepsch, Hans v., et al. "Complex Domain Architecture of Multicompartment Micelles from a Linear ABC Triblock Copolymer Revealed by Cryogenic Electron Tomography." Chemical Communications, no. 17, 2009, pp. 2290–2292., https://doi.org/10.1039/b903658j.

34. Kyeremateng, Samuel Oppong, et al. "Synthesis of ABC and Cabac Triphilic Block Copolymers by ATRP Combined with 'Click' Chemistry." *Macromolecular Rapid*

Communications, vol. 29, no. 12–13, 2008, pp. 1140–1146., https://doi.org/10.1002/marc.200800058.

35. He, Jinlin, et al. "Synthesis and Characterization of Amphiphilic Fluorinated Pentablock Copolymers Based on Pluronic F127." *Journal of Polymer Science Part A: Polymer Chemistry*, vol. 46, no. 9, 2008, pp. 3029–3041., https://doi.org/10.1002/pola.22641.

36. Kaberov, Leonid I., et al. "Fluorophilic–Lipophilic–Hydrophilic Poly(2-Oxazoline) Block Copolymers as MRI Contrast Agents: From Synthesis to Self-Assembly." *Macromolecules*, vol. 51, no. 15, 2018, pp. 6047–6056., https://doi.org/10.1021/acs.macromol.8b00957.

37. Kubowicz, Stephan, et al. "Multicompartment Micelles Formed by Self-Assembly of Linear ABC Triblock Copolymers in Aqueous Medium." *Angewandte Chemie International Edition*, vol. 44, no. 33, 2005, pp. 5262–5265., https://doi.org/10.1002/anie.200500584.

38. Tan, Xiao, et al. "Amphiphilic Perfluoropolyether Copolymers for the Effective Removal of Polyfluoroalkyl Substances from Aqueous Environments." *Macromolecules*, vol. 54, no. 7, 2021, pp. 3447–3457., https://doi.org/10.1021/acs.macromol.1c00096.

39. Sundaram, Harihara S., et al. "Fluorinated Amphiphilic Polymers and Their Blends for Fouling-Release Applications: The Benefits of a Triblock Copolymer Surface." *ACS Applied Materials & Interfaces*, vol. 3, no. 9, 2011, pp. 3366–3374., https://doi.org/10.1021/am200529u.

40. Ishizone, Takashi, et al. "Anionic Polymerizations of Perfluoroalkyl Methacrylates and Synthesis of Well-Defined ABC Triblock Copolymers of Methacrylates Containing Hydrophilic, Hydrophobic, and Perfluoroalkyl Groups." *Polymer Journal*, vol. 31, no. 11_2, 1999, pp. 983–988., https://doi.org/10.1295/polymj.31.983.

41. Barres, Alexa R., et al. "Multicompartment Theranostic Nanoemulsions Stabilized by a Triphilic Semifluorinated Block Copolymer." *Molecular Pharmaceutics*, vol. 14, no. 11, 2017, pp. 3916–3926., https://doi.org/10.1021/acs.molpharmaceut.7b00624.

42. Hillmyer, Marc A., and Timothy P. Lodge. "Synthesis and Self-Assembly of Fluorinated Block Copolymers." *Journal of Polymer Science Part A: Polymer Chemistry*, vol. 40, no. 1, 2001, pp. 1–8., https://doi.org/10.1002/pola.10074.

43. Lin, Chen Xiao, et al. "Anion Conductive Triblock Copolymer Membranes with Flexible Multication Side Chain." *ACS Applied Materials & Interfaces*, vol. 10, no. 21, 2018, pp. 18327–18337., https://doi.org/10.1021/acsami.8b03757.

44. Stefik, Morgan, et al. "Networked and Chiral Nanocomposites from ABC Triblock Terpolymer Coassembly with Transition Metal Oxide Nanoparticles." *J. Mater. Chem.*, vol. 22, no. 3, 2012, pp. 1078–1087., https://doi.org/10.1039/c1jm14113a.

45. Sarkar, Amrita, et al. "Expanded Kinetic Control for Persistent Micelle Templates with Solvent Selection." *Langmuir*, vol. 34, no. 20, 2018, pp. 5738–5749., https://doi.org/10.1021/acs.langmuir.8b00417.

46. "Polymers." *Polymer Database*, 2015, https://polymerdatabase.com/.

47 Barton, Allan F. "Solubility Parameters." *Chemical Reviews*, vol. 75, no. 6, 1975, pp. 731–753., https://doi.org/10.1021/cr60298a003.

48. Tsutsumi, Shinichi, et al. "Functional Composite Material Design Using Hansen Solubility Parameters." *Results in Materials*, vol. 4, 2019, p. 100046., https://doi.org/10.1016/j.rinma.2019.100046.

49. Hinze, G., et al. "Anisotropic Motion of Toluene above and below the Glass Transition Studied by 2H NMR." *Chemical Physics Letters*, vol. 232, no. 1-2, 1995, pp. 154–158., https://doi.org/10.1016/0009-2614(94)01322-m.

50. Lesikar, Arnold V. "Effect of Association Complexes on the Glass Transition in Organic Halide Mixtures." *The Journal of Physical Chemistry*, vol. 80, no. 9, 1976, pp. 1005–1011., https://doi.org/10.1021/j100550a018.

51. "Milliporesigma." *MilliporeSigma | Life Science Products & Service Solutions*, 2022, https://www.sigmaaldrich.com/US/en/product/aldrich/196916.

52. www.Hansen-Solubility.com. "HSP Examples: Poly Lactic Acid (PLA)." *HSP Examples: PLA | Hansen Solubility Parameters*, 2022, https://www.hansen-solubility.com/HSP-examples/pla.php.

53. Su, Shen. "Prediction of the Miscibility of PBAT/PLA Blends." *Polymers*, vol. 13, no. 14, 2021, p. 2339., https://doi.org/10.3390/polym13142339.

54. Lewis, Sally E., et al. "Upcycling Aromatic Polymers through C–H Fluoroalkylation." *Chemical Science*, vol. 10, no. 25, 2019, pp. 6270–6277., https://doi.org/10.1039/c9sc01425j.

55. Liu, Hanbin, et al. "Solvent-Driven Formation of Worm-like Micelles Assembled from a Co2-Responsive Triblock Copolymer." *Langmuir*, vol. 31, no. 32, 2015, pp. 8756–8763., https://doi.org/10.1021/acs.langmuir.5b00885.

56. Sarkar, Amrita, et al. "Polarclean & Dimethyl Isosorbide: Green Matches in Formulating Cathode Slurry." *Energy Advances*, vol. 1, no. 10, 2022, pp. 671–676., https://doi.org/10.1039/d2ya00161f.

57. Rajput, Faraz, et al. "Poly (Styrene/Pentafluorostyrene)-Block-Poly (Vinyl Alcohol/Vinylpyrrolidone) Amphiphilic Block Copolymers for Kinetic Gas Hydrate Inhibitors: Synthesis, Micellization Behavior, and Methane Hydrate Kinetic Inhibition."

Journal of Polymer Science Part A: Polymer Chemistry, vol. 56, no. 21, 2018, pp. 2445–2457., https://doi.org/10.1002/pola.29219.

58. Fedors, Robert F. "A Method for Estimating Both the Solubility Parameters and Molar Volumes of Liquids." *Polymer Engineering and Science*, vol. 14, no. 2, 1974, pp. 147–154., https://doi.org/10.1002/pen.760140211.

59. Sarkar, Amrita, and Stefik Morgan. "Robust Porous Polymers Enabled by a Fast Trifluoroacetic Acid Etch with Improved Selectivity for Polylactide." *Materials Chemistry Frontiers*, vol. 1, no. 8, 2017, pp. 1526–1533., https://doi.org/10.1039/c6qm00266h.

60. Jakubowski, Wojciech, et al. "Polystyrene with Improved Chain-End Functionality and Higher Molecular Weight by Arget ATRP." *Macromolecular Chemistry and Physics*, vol. 209, no. 1, 2008, pp. 32–39., https://doi.org/10.1002/macp.200700425.

61. Todd, Richard, et al. "Poly(ω-Pentadecalactone)-*b*-Poly(l-Lactide) Block Copolymers via Organic-Catalyzed Ring Opening Polymerization and Potential Applications." *ACS Macro Letters*, vol. 4, no. 4, 2015, pp. 408–411., https://doi.org/10.1021/acsmacrolett.5b00021.

62. Kumar, Arun, et al. ``Rop and ATRP Fabricated Dual Targeted Redox Sensitive Polymersomes Based on PPEGMA-PCL-SS-PCL-PPEGMA Triblock Copolymers for Breast Cancer Therapeutics." *ACS Applied Materials & Interfaces*, vol. 7, no. 17, 2015, pp. 9211–9227., https://doi.org/10.1021/acsami.5b01731.

63. Jankova, Katja, and Søren Hvilsted. "Preparation of Poly(2,3,4,5,6-Pentafluorostyrene) and Block Copolymers with Styrene by ATRP." *Macromolecules*, vol. 36, no. 5, 2003, pp. 1753–1758., https://doi.org/10.1021/ma021039m.